

A numerical procedure based on a hierarchical fiber-bundle model.

Scaling Properties of Nanotube-Based Macroscopic Cables Through Multiscale Numerical Simulations



© DIGITAL VISION

CARBON NANOTUBE (CNT) BUNDLES ARE EXTREMELY interesting for engineering applications because of their density, elastic modulus, and mechanical strength [1], [2]. In particular, ambitious structures such as space elevators [3]–[5] or superbridges [6] (i.e., kilometer-long suspended bridges) could be conceived by exploiting the unique properties provided by CNT technology.

Many experimental studies exist for the evaluation of the mechanical characteristics of CNTs or CNT yarns [7]; however, numerical studies clearly become indispensable when predictions are to be made for full-scale structures [8]. Due to the number of orders of magnitude involved, which can be up to ten in the case of superbridges or even 15 in the case of a space-elevator megacable, problems often emerge because of the computing time or complexity involved. Inevitably, a

NICOLA PUGNO AND FEDERICO BOSIA

Digital Object Identifier 10.1109/MNANO.2009.934863

statistical approach is called for, and the issue is then to consider all relevant parameters and choose appropriate approximations for the problem to be analyzed. In this respect, the role played by defects in the structure at various levels is of utmost importance, especially in the determination of the final bundle strength [5].

To address these issues, we describe a numerical procedure based on a hierarchical fiber-bundle model (HFBM) [8] approach specifically developed to carry out multiscale simulations for CNT-based cables and estimate relevant mechanical characteristics such as Young's modulus, strength or released energy during damage progression, and evaluate the scaling of these properties with cable size.

NUMERICAL MODEL AND MULTISCALE APPROACH

MODEL

Simulations are carried out using a recently developed simulation code for the description of damage progression and acoustic emission (AE) in materials [4], [8]. The simulation code is based on an equal-load-sharing FBM approach [9], with randomly assigned (Weibull-distributed) fiber strengths σ_{Cij} . The specimen is modeled by adopting a discretization in N_x bundles of N_y fibers (corresponding to CNTs or CNT bundles) and by applying at every time step the analytically calculated local loads deriving from an increasing externally applied stress $\sigma(t)$. An AE event is generated whenever this local stress exceeds the assigned fiber peak stress. In this case, the corresponding fiber stiffness k_{ij} is set to zero, and the related section (or bundle) undergoes a corresponding stiffness reduction.

Energy dissipation owing to the formation of new fracture surfaces at each AE event is also accounted for in the formulation: energy balance requires that the variation of total potential energy $\Delta U_{ij}(t)$, when an AE event occurs at the location (i, j) , needs to be compensated by the kinetic energy $\Delta T_{ij}(t)$ (released in the form of a stress wave) and dissipated energy $\Delta \Omega_{ij}(t)$ (formation of a crack surface at micro- or mesoscale). Thus, we can write

$$\Delta U_{ij}(t) + \Delta T_{ij}(t) + \Delta \Omega_{ij}(t) = 0. \quad (1)$$

Many experimental studies exist for the evaluation of the mechanical characteristics of CNTs or CNT yarns.

The potential energy variation $\Delta U_{ij}(t)$ is related to the imposed displacement $x(t)$, and the overall specimen stiffness variation $\Delta K_{ij}(t)$ occurring in correspondence with the AE event

$$\Delta U_{ij}(t) = \frac{1}{2} x(t)^2 \Delta K_{ij}(t), \quad (2)$$

whereas the dissipated energy $\Delta \Omega_{ij}$ is assumed to be proportional to the newly created crack surfaces A_{ij}

$$\Delta \Omega_{ij} = G_C A_{ij}, \quad (3)$$

where G_C is the critical strain energy release rate of the material. The surfaces A_{ij} can be considered constant as a first approximation and correspond to CNT cross sections in the lowest simulation level.

MULTISCALE SIMULATION PROCEDURE

To tackle the size scales involved in the modelization of CNT megacables, spanning up to approximately 15 orders of magnitude from CNT ($\sim 10^{-7}$ m) to megacable lengths, the HFBM [8] outlined earlier must be modified to accommodate multiscale simulations. The cable is therefore modeled as a N_{xk} by N_{yk} ensemble of subvolumes, arranged in parallel sections, as shown

in Figure 1. Each of the (primary) subvolumes is in turn constituted by $N_{x(k-1)}$ by $N_{y(k-1)}$ (secondary) subvolumes, arranged in parallel as before. This scheme is applied for k generations, down to a level 1 subvolume, which is constituted by a N_{x1} by N_{y1} arrangement of springs or fibers representing the actual CNT (Figure 1). Here, we adopt a scale-invariant approach, whereby the simulated structure appears the same at any given scale level (i.e., the length/width ratio is constant) and therefore $N_{x1} = N_{x2} = \dots = N_{xk} = N_x$ and $N_{y1} = N_{y2} = \dots = N_{yk} = N_y$. Overall, the cable is constituted by a total number of CNTs given by $N_{\text{tot}} = (N_x N_y)^k$. In silico hierarchical experiments have been carried out according to the following scheme:

- 1) Simulations at level 1:
 - ◆ the CNTs (or fibers in the model) are assigned a fixed elastic modulus and random failure strength using a (nanoscale) Weibull statistical distribution, derived from observations on nanotensile tests of CNTs [10]
 - ◆ linearly increasing strains are applied to the fiber bundle and at each code iteration the number of fractured fibers is

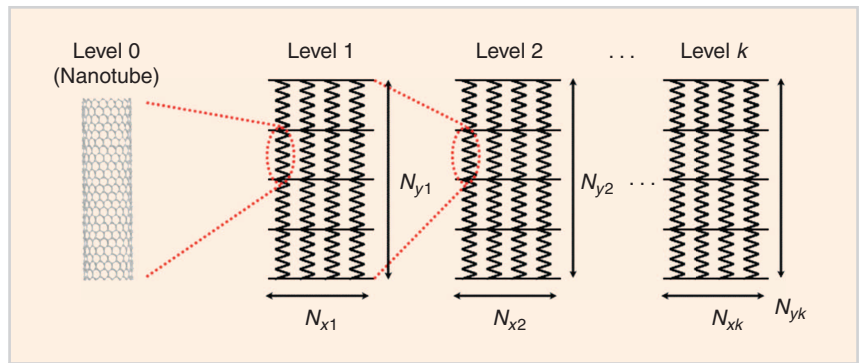


FIGURE 1 Schematization of the adopted multiscale simulation procedure to determine CNT megacable mechanical characteristics.

The simulation code is based on an equal-load-sharing FBM approach, with randomly assigned (Weibull-distributed) fiber strengths.

computed (fracture occurs when local stress exceeds the CNT failure strength), and the strains are uniformly redistributed among the remaining intact fibers in each section (the uniform redistribution is plausible for independent CNTs. In any case, a stress concentration can be included in our model and would further reduce the failure stress)

- ◆ various quantities versus time are monitored during the simulation, e.g., stress-strain, Young's modulus, number and location of fractured fibers, kinetic energy emitted, fracture energy absorbed, among others. The simulation terminates when all fibers in one of the sections become fractured, separating the cable into two pieces
 - ◆ the above procedure is repeated many times to obtain reliable statistics for the various computed quantities, usually 10^3 – 10^4 times for each level.
- 2) Simulations at level 2 up to k :
- ◆ the second-level fibers are those characterized in level 1 simulations, i.e., their stiffness and strength distribution are derived from level 1 results. The same is true for level 3 simulations depending on level 2 results and so on. This means that the elastic modulus and the statistical distribution of the failure stress of level k fibers are assigned according to those emerging from level $k-1$ simulations; again, repeated displacement-controlled virtual experiments are carried out at each level, with the same procedure as that outlined for

level 1, leading hierarchically, at level k , to results for the full-scale CNT megacable.

In this approach, we assume that the end-to-end connections in nanotubes and nanotube bundles have a strength comparable to that of nanotubes or bundles themselves, assuming a long-enough overlap length. With this assumption, we expect to obtain an upper-bound estimation for the overall cable strength.

ROLE OF DEFECTS

As explained earlier, any numerical simulation regarding the mechanical characteristics of CNTs or CNT bundles without considering the role of defects would be unrealistic [4], [5]. Defects can occur both at the atomic level and larger scale sizes when single-fractured CNTs or fractured CNT bundles are present. These defects (or voids) can be introduced in the simulations by setting local fiber stiffnesses k_{ij} to zero at selected locations and levels. For simplicity, we consider only uniformly distributed defects (with a void density of 10% occurring at all simulation levels) or clustered defects, i.e., circular defects whose width is one tenth of the bundle width occurring at level 1 and also occurring with overall void density of 10%. This percentage can probably be expected to be an upper limit in void concentration, at least at an atomic level [11].

NUMERICAL RESULTS

DAMAGE EVOLUTION

The first simulation is carried out at CNT level, i.e., the fibers in the first-generation subvolume are $L_0 = 10^{-7}$ m in length. This length value is not necessarily the CNT length, but rather it represents a sort of correlation length, i.e., the distance beyond which a CNT rupture does not influence other ruptures in

the bundle. The fibers are $m_0 = 10^{-9}$ m in width, their Young's modulus is $E_0 = 10^{12}$ Pa, and their strength σ_{f0} is randomly assigned, based on the nano-scale Weibull [10] distribution

$$P(\sigma_{f0}) = 1 - \exp[-(\sigma_{f0}/\sigma_0)^n], \quad (4)$$

where P is the cumulative probability, and experimentally, $\sigma_0 = 34$ GPa and $m \approx 3$ for CNTs. This distribution accounts for the statistical variations in CNT strength that is to be expected for various reasons, including the presence of defects in CNTs. However, the fiber bundle is considered defect free at all levels, i.e., all fibers are present in the grid used in the simulations. The strength σ_{f1} of the first-generation fiber bundle (whose length is $L_1 = L_0 N_{y1}$) is then derived as the average value of those deriving from a large number of repeated simulations (typically from 10^3 to 10^4), each with different randomly assigned local strengths so as to build reliable statistics.

In contrast, the strengths of the fiber bundles at level 2 upward (σ_{f2} to σ_{fk}), as explained earlier, are directly deduced from the numerically simulated distribution of strengths obtained at the previous level in each case. The strength σ_{fk} coincides with the final strength σ_f of the considered structure. Here, the results are presented for simulations with $N_y/N_x = 25$ and $k = 1 \dots 15$, so that $L(k+1)/L(k) = 10$ for all k .

Figure 2 shows the stress-strain behavior obtained when defective or nondefective bundles of total length $L = 10^3$ m are considered. Brittle fracture is observed for a strain level of about 1.2% in the case of a nondefective cable. The fracture strain (and, consequently, fracture stress) is reduced by about 15% in the case of a cable with distributed level 1 defects and a further 15% in the case of circular defects (whose configuration is described in the previous section). Correspondingly, a slight stiffness reduction is observed.

The effect of defects in the CNT bundle structure can be visualized in Figure 3, where fracture maps (i.e., the spatial distribution of damaged fibers) are shown at the start of the simulation ($t = 0$) and at specimen failure ($t = t_f$) in the case of a cable where a circular defect

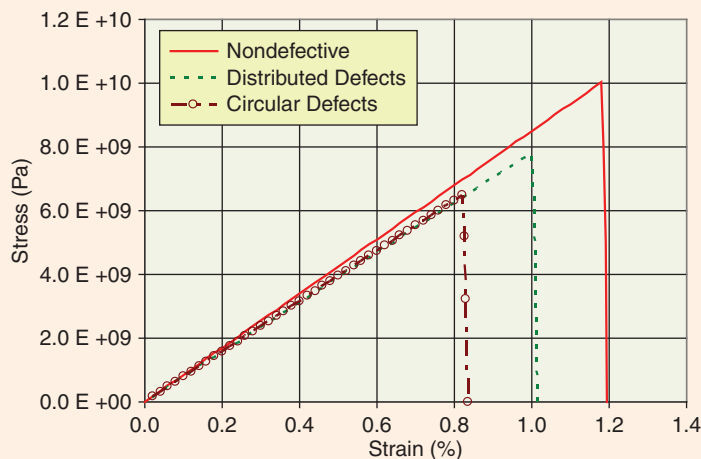


FIGURE 2 Stress–strain curves for CNT bundles up to rupture in the case of nondefective and defective cables. The types of defects considered are described in the text.

is initially present. The figure shows that cracks tend to propagate in cable sections, where defects are initially present because of stress concentrations.

SCALING OF CNT-CABLE STIFFNESS AND STRENGTH

The procedure outlined in the “Numerical Model and Multiscale Approach” section allows us to study the scaling of stiffness and strength with CNT cable length as well as evaluate the influence of the presence of defects. Scaling is assessed more than 15 orders of magnitude, from 10^{-7} m to 10^8 m (the latter being the space-elevator megacable length), although only values of up to $\sim 10^3$ m are of practical interest for civil engineering applications. Figure 4 shows the results for the scaling of normalized cable stiffness E/E_0 and Figure 5 for the normalized cable strength σ/σ_0 . Both stiffness and strength decrease with increasing cable length. The main decrease occurs for small lengths ($< 10^{-4}$ m) and then continues with an almost linear (in log scale) drop-off for larger abscissa. Various analytical laws for this behavior have been proposed by the authors [4], [12], [13]. Cable strength estimations, herein, are in good agreement with those derived from these analytical laws. The reduction with increasing cable length is particularly significant for strength (75% over the 15 orders of magnitude), while the stiffness decreases only about 15% over the same length range.

As mentioned earlier, the presence of defects causes a nonnegligible decrease in cable stiffness, with a 9% overall reduction in the case of a randomly distributed 10% void content. In this case, the effect of defect clustering is less pronounced, i.e., the stiffness reduction in the case of clustered circular defects (with an overall 10% concentration) is virtually the same as that for randomly distributed defects. On the other hand, the presence of defects has a more consistent effect on the decrease of cable strength, with a further 13% reduction with respect to the nondefective value in the case of distributed defects, and a 29%

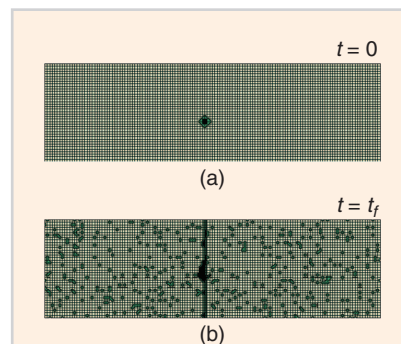


FIGURE 3 (a) Spatial distribution of damage in a model CNT cable portion with an initial defect (at $t = 0$). (b) Clustering of defects in the specimen section, where damage already present can be observed till failure is reached at $t = t_f$.

reduction in the case of clustered circular defects. These simulations show how defects of nonnegligible size have a more pronounced effect in reducing cable strength with the same overall concentration, whereas in the case of cable stiffness, it is mainly the defect concentration that plays a role.

ENERGY SCALING

Another important quantity to consider when evaluating scaling properties of CNT bundles is the released energy during the damaging process, normally occurring in the form of stress waves (AE). The latter can be detected experimentally in simple, nondestructive tests, using sensors

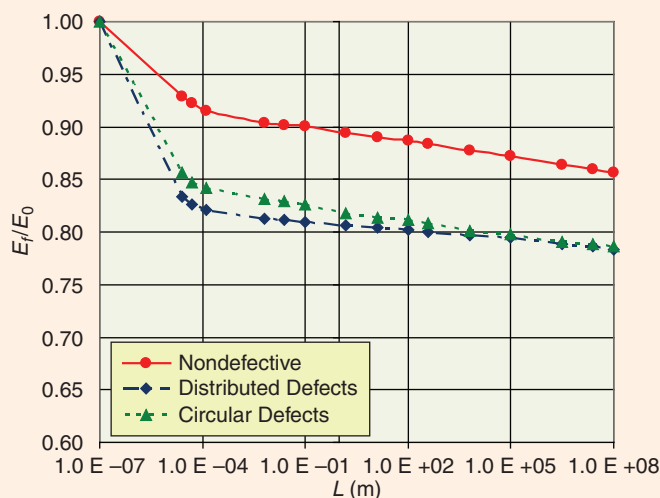


FIGURE 4 Numerically computed normalized cable stiffness E/E_0 versus specimen length L in the case of nondefective and defective CNT cables.

An important quantity to consider when evaluating scaling properties of CNT bundles is the released energy during the damaging process.

attached to the structure at various locations and the data used for health monitoring. Ideally, potentially critical conditions could be detected prior to failure using the detected data in real time. However, AE energy does not scale trivially with

time or with specimen size, and therefore, analytical and numerical data are necessary to correctly interpret experimental data relative to full-scale structures.

As explained earlier and documented elsewhere [8], the present model accounts

for the dissipated energy in crack surface formation and yields results that are consistent with the experimental results from AE tests used to characterize damage progression in materials. In particular, fracture avalanches are correctly reproduced, with the avalanches occurring due to the load transfer from broken to intact fibers in the course of loading. Specific distributions for these avalanches are known for different HFEBMs [8], namely an asymptotic power-law distribution with exponent $-5/2$ occurring in the majority of cases [9]. The present model also yields a power-law distribution for released AE energy T

$$P(T) \propto T^\alpha \quad (5)$$

with an exponent α , which typically varies between -1.6 and -2.1 depending on the chosen parameters (mainly, the chosen Weibull modulus m). Typical results are shown in Figure 6 for the mechanical parameters used in level 1 simulations in the “Model” subsection and $G_C = 10 \text{ J/m}^2$. Here, the cumulative distribution $N(T)$ is shown. The scaling exponent is $\alpha = -1.9$. This and other numerically computed exponents (see [14] and references therein) differ from the $-5/2$ value but are closer to the experimental values found in literature. It has been suggested [14] that this power-law behavior could be indicative of an underlying critical dynamics of the process, related to the absence of a characteristic length and a self-similarity in the microfracturing phenomenon.

Using the described multiscale simulation procedure, the scaling of the released energy T can now be determined as a function of CNT cable length. Results are shown in Figure 7. A power-law increase (linear behavior in log-log scale) is found, similar to previous results relative to different materials [6]. Results in Figure 7, however, are obtained in a much greater length range, showing the advantages of the adopted multiscale simulation procedure.

CONCLUSIONS

We have presented numerical simulations based on a modified HFEBM [8] approach, with due consideration for energy dissipation and a multiscale procedure to determine scaling properties of CNT megacables in a wide length range.

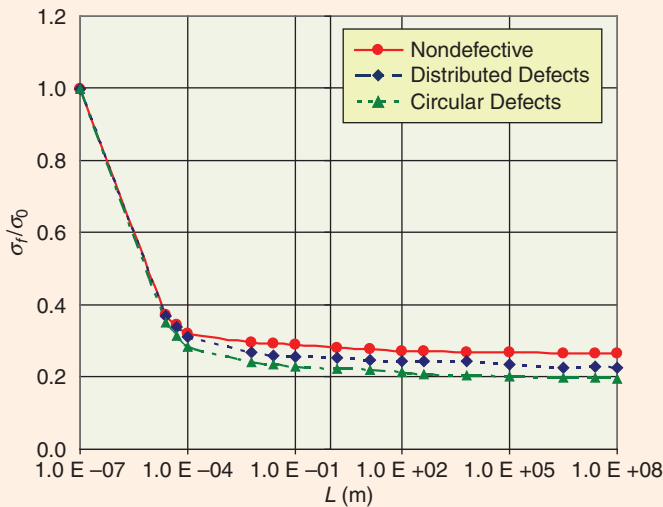


FIGURE 5 Numerically computed normalized cable strength σ_f/σ_0 versus specimen length L in the case of nondefective and defective CNT cables.

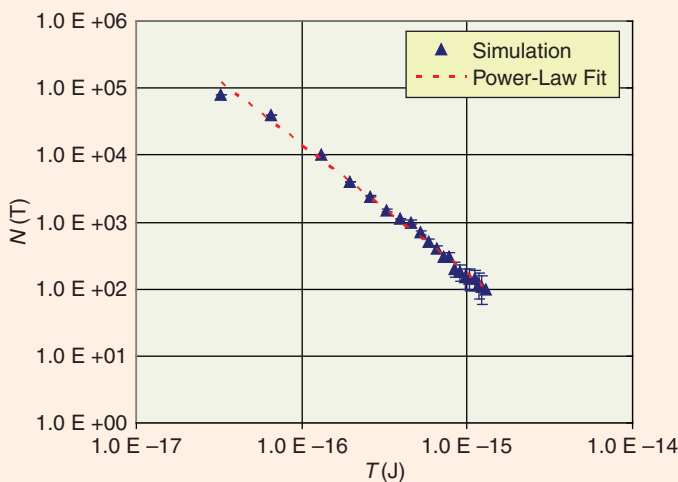


FIGURE 6 Released energy distribution $N(T)$ at level 1. A power-law fit is included for comparison.

Defects can occur both at the atomic level and larger scale sizes when single-fractured CNTs or fractured CNT bundles are present.

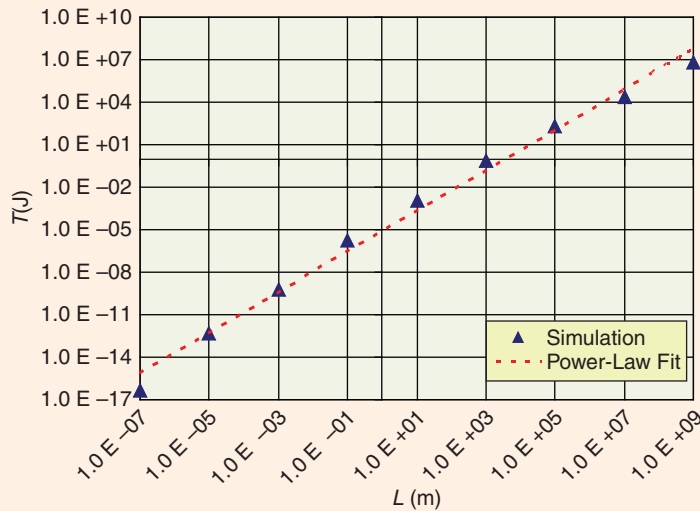


FIGURE 7 Numerically computed scaling properties of AE energy T . A power-law fit is included.

Analyzed properties include strength, stiffness, and released AE energy. The effect of defects on the cable stiffness and strength is discussed. Results show consistent reductions of strength with cable length and, to a lesser extent, of stiffness, and in both cases, the presence of defects is found to be nonnegligible. Power-law type behavior is found for energy scaling, similar to existing experimental and numerical results in the literature, but in this case, relative to a much greater length range. The numerical procedure shows promise and could in future be used in specific detailed studies on CNT-cable applications.

ACKNOWLEDGMENTS

Nicola Pugno is supported by Bando regionale Converging Technologies, Biotechnology—Nanotechnology, METREGEN 2008, “Metrology on a cellular and macromolecular scale for regenerative medicine.”

ABOUT THE AUTHORS

Nicola Pugno (nicola.pugno@polito.it) received his degrees in mechanical

engineering and theoretical physics and his Ph.D. (fracture mechanics) degree in structural engineering. He previously served as an associate professor of structural mechanics. He is currently a professor of structural bio- and nanomechanics. He has presented approximately 200 papers in international journals and conference proceedings.

Federico Bosia (fbosia@to.infn.it) is with the Department of Theoretical Physics, University of Torino, in Italy.

REFERENCES

- [1] K. Koziol, J. Vilatela, A. Moisala, M. Motta, P. Cuniff, M. Sennett, and A. Windle, “High-performance carbon nanotube fiber,” *Science*, vol. 318, no. 5858, pp. 1892–1895, 2007.
- [2] M. F. Yu, O. Lourie, M. J. Dyer, K. Moloni, T. F. Kelly, and R. Ruoff, “Strength and breaking mechanism of multiwalled carbon nanotubes under tensile load,” *Science*, vol. 287, no. 5453, pp. 637–640, 2000.
- [3] B. C. Edwards, “Design and deployment of a space elevator,” *Acta Astronaut.*, vol. 10, no. 10, pp. 735–744, 2000.
- [4] N. Pugno, “On the strength of the nanotube-based space elevator cable: From nanomechanics to megamechanics,” *J. Phys. Condens. Matter*, vol. 18, pp. S1971–S1990, 2006.
- [5] N. Pugno, “The role of defects in the design of the space elevator cable: From nanotube to megatube,” *Acta Mater.*, vol. 55, pp. 5269–5279, 2007.

- [6] A. Carpinteri and N. Pugno, “Super-bridges suspended over carbon nanotube cables,” *J. Phys. Condens. Matter*, vol. 20, no. 474213, pp. 1–8, 2008.
- [7] M. Zhang, K. R. Atkinson, and R. H. Baughman, “Multifunctional carbon nanotube yarns by downsizing an ancient technology,” *Science*, vol. 306, no. 5700, pp. 1358–1361, 2004.
- [8] N. Pugno, F. Bosia, and A. Carpinteri, “Multiscale stochastic simulations as in-silico tensile testing of nanotube-based macroscopic cables,” *Small*, vol. 4, no. 8, pp. 1044–1052, 2008.
- [9] F. Kun, S. Zapperi, and H. J. Herrmann, “Damage in fiber bundle models,” *Eur. Phys. J. B*, vol. 17, no. 2, pp. 269–279, 2000.
- [10] N. Pugno and R. Ruoff, “Nanoscale Weibull statistics,” *J. Appl. Phys.*, vol. 99, no. 1, pp. 024301–024301-4, 2006.
- [11] J. Yuana and K. M. Liewa, “Effects of vacancy defect reconstruction on the elastic properties of carbon nanotubes,” *Carbon*, vol. 47, no. 6, pp. 1526–1533, 2009.
- [12] N. Pugno, “Space elevator: Out of order?” *Nano Today*, vol. 2, no. 6, pp. 44–47, 2007.
- [13] A. Carpinteri, “Scaling laws and renormalization group for strength and toughness of disordered materials,” *Int. J. Sol. Struct.*, vol. 31, no. 3, pp. 291–302, 1994.
- [14] A. Petri, G. Paparo, A. Vespignani, A. Alippi, and M. Costantini, “Experimental evidence for critical dynamics in microfracturing processes,” *Phys. Rev. Lett.*, vol. 73, no. 25, pp. 3423–3426, 1994.

N



IEEE JobSite
The Right Candidate - Right Now!

Take the next steps to finding your ideal job.

The IEEE Job Site can help you explore the engineering career opportunities that may be right for you.

Take advantage of this unique member benefit.

Create a personal, confidential job profile, post your resumé and start your job search now!

Visit the IEEE Job Site at www.ieee.org/jobs

